New measurements of the intensity and geometrical structure of the upwelling and downwelling underwater light fields (radiance distributions)

David Antoine[1], Edouard Leymarie[1], André Morel[1], Amel Houyou[1,2], Stéphane Victori[2], Didier Crozel[2], and Bertrand Fougnie[3]

[1]*Laboratoire d'Océanographie de Villefranche (CNRS-LOV), Villefranche sur mer, France,*
[2]*CIMEL Electronique, Paris, France,*
[3] *Centre National d'Etudes Spatiales (CNES), Toulouse, France*

Outline

- ✓ What do we call the underwater “radiance distribution”?
- ✓ Why measuring radiance distributions?
- ✓ What was done before?
- ✓ Our new development (new “radiance camera”; description; characterization, deployment modes)
- ✓ Sample results (surface and vertical profiles)
- ✓ Validation against more classical “off-the-shelf” radiometers
- ✓ Tentative inversion of radiance distributions in terms of optical properties: method and results
- ✓ Conclusions / perspectives

What do we call the “radiance distribution”?

✓ Below the air-sea interface, the radiant flux experiences scattering and absorption within the water column.

✓ There is accordingly a redistribution of energy in all directions.

✓ This is determined by boundary conditions (radiance distribution just above the surface, and the state of the air-sea interface), and by the inherent optical properties (IOPs), i.e., absorption (a) and the volume scattering function (VSF, of $\beta(\theta)$)

Radiance, L, “*Radiant flux in a given direction per unit solid angle per unit projected area*”

✓ $L(\theta,\phi)$ for θ from 0 to π, and for ϕ from 0 to 2π, will be referred to as $L(\Xi)$
✓ Radiances travelling downward for $\theta=\pi$ are referred to as nadir radiances

✓ The distribution for the upward hemisphere (downwelling radiances): $L(\Xi_d)$
✓ The distribution for the downward hemisphere (upwelling radiances): $L(\Xi_u)$

Why measuring L(Ξ)?

Two main objectives:

Fundamental:
Better characterization / understanding of L(Ξ). The vertical structure of the underwater light field is important for biology (photosynthesis) and physics (heating rate).

More applied:
1 - L(Ξ) determines the distribution of radiances escaping the ocean, i.e., the water-leaving radiances (L_w) that we measure from space with so-called "ocean color" remote sensing satellites.
It is, therefore, necessary to know L(Ξ) (at least L($Ξ_u$)) in order to know how L_w's are distributed over space (normalization of observations taken under various sun elevations and different view angles; data merging)
Well characterized for open ocean waters (at least just beneath the sea surface); totally undocumented for coastal turbid waters

2 - An accurate knowledge of depth changes of L(Ξ) within the water column in principle gives access to all optical properties (through inversion procedures); this would be a sort of "generic" or "universal" measurement.

What was done before?

Jerlov N.G. and M. Fukuda, 1960,
Tellus 12, 348-355

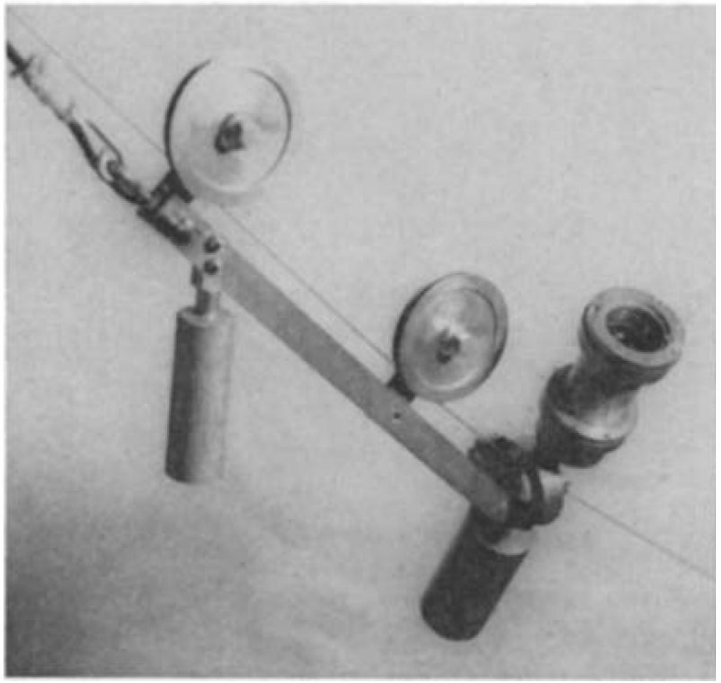

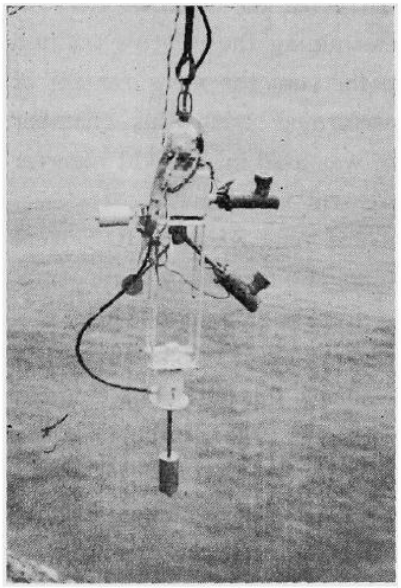

Fig. 1. The submerged unit before lowering.

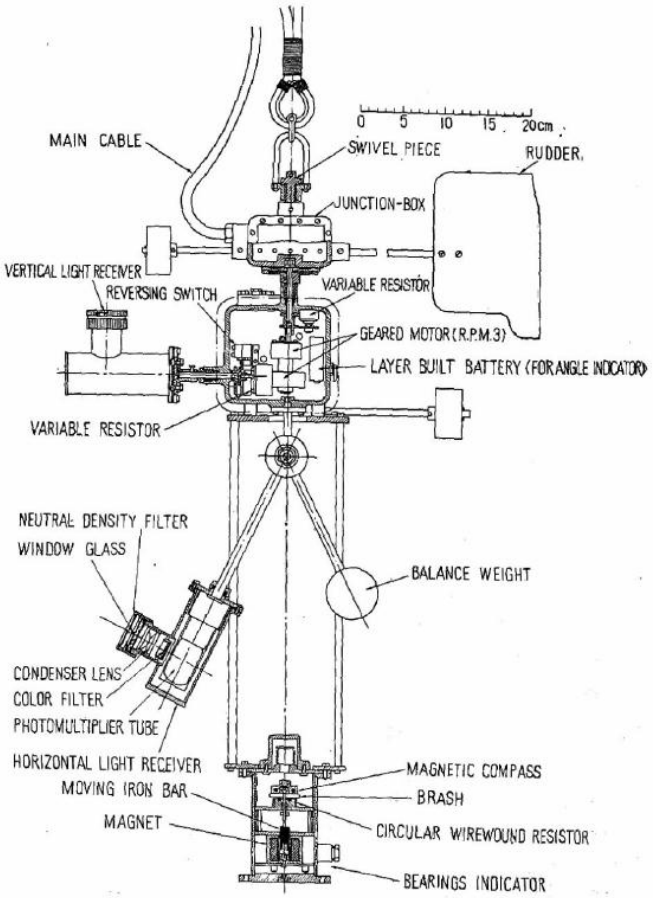

Fig. 2. General arrangement of the submerged unit.

Sasaki T. et al., 1962, Bull. Jap. Soc. Sci. Fish.
28(5), 489-496

What was done before?

John E. Tyler, 1960, Bull. Scripps Inst. Oceanogr. 7, 363-412.

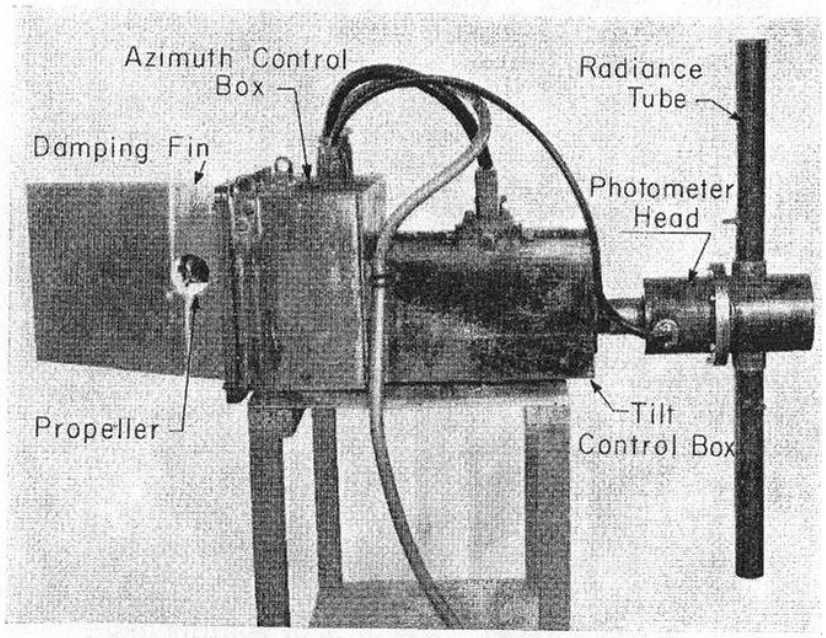

Fig. 8. Underwater radiance photometer (Tyler, 1960). The measuring head with its radiance tubes is on the right. The center box holds the tilt motor. The left box contains the gyrosyn compass and propeller-drive motor. The propeller can be seen through a hole in the damping fin on the left.

The Sea, Vol 1., M. N. Hill Ed., (1962)

Unidirectional photometer with elevation scanning

Radiances distribution in Lake Pend'Oreille
Redrawn from the data published by Tyler, 1960

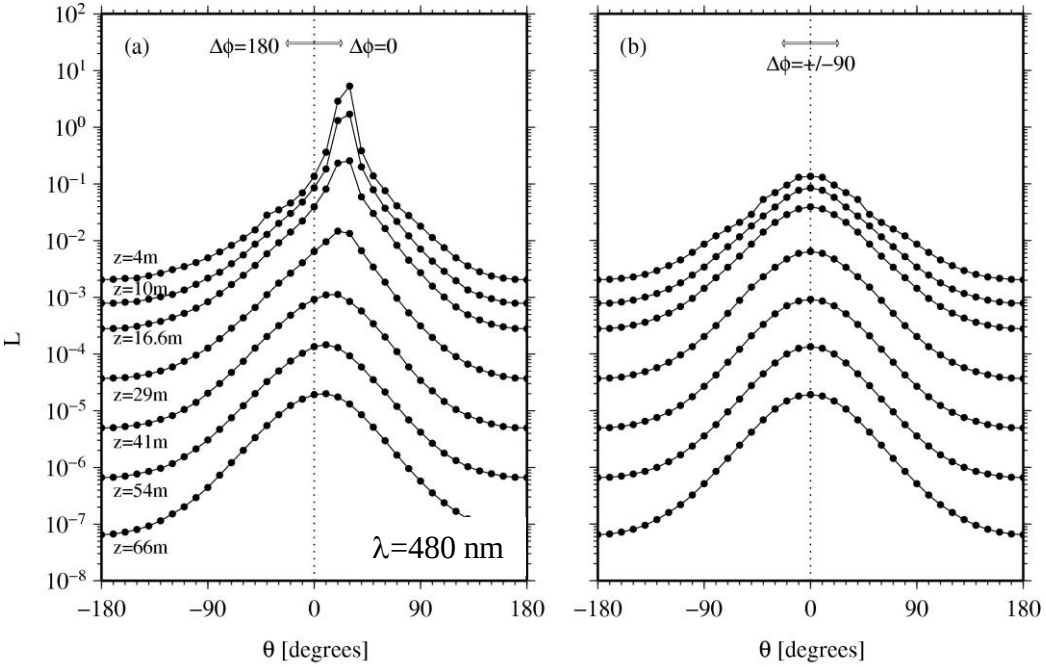

Principal plane

Perpendicular plane

Previous developments, cont'd

R.C. Smith 1970 : Fish Eye camera

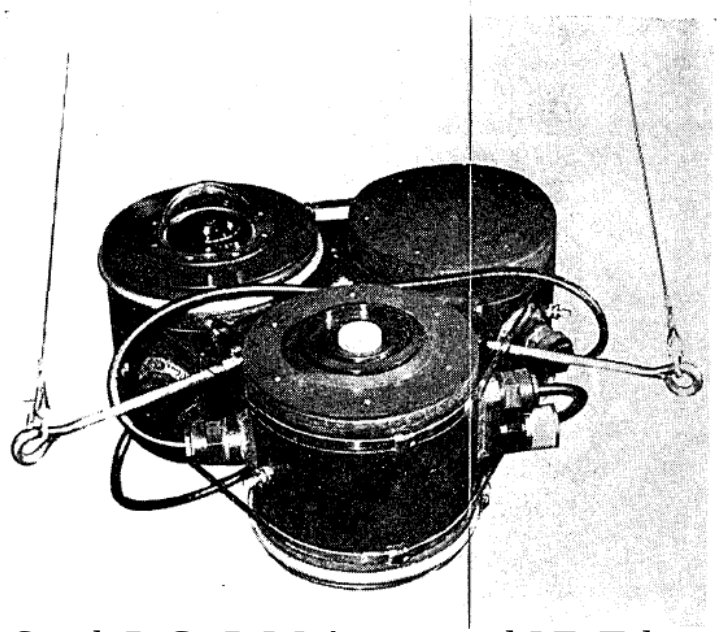

Smith R.C., R.W. Austin, and J.E. Tyler, 1970.
An oceanographic radiance distribution camera system, Applied Optics 9(9), 2015-2022

(Vis. Lab at Scripps)

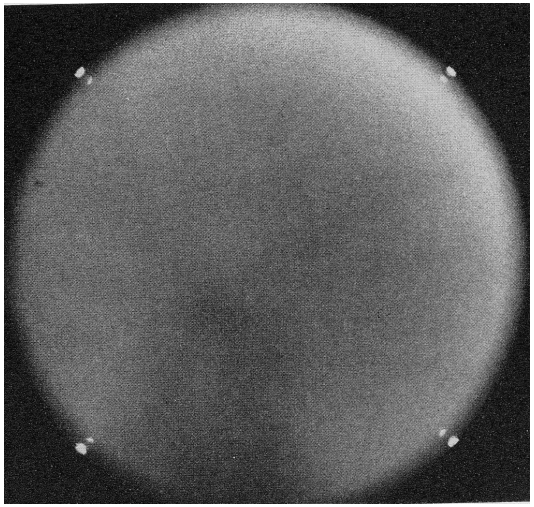

Upwelling radiances

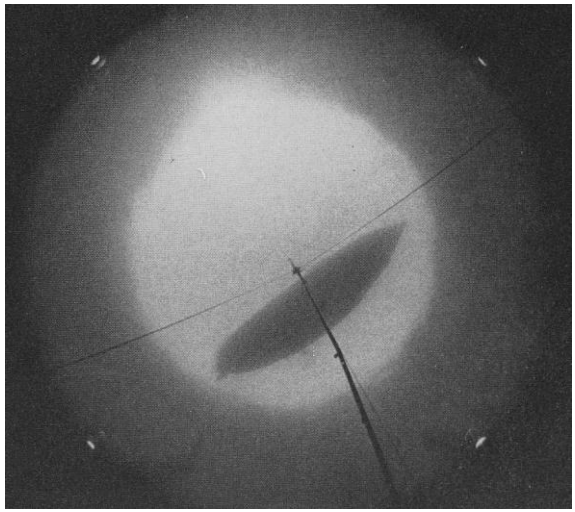

downwelling radiances

(Med. Sea 1972)

Optical Aspects of Oceanography,
N.G. Jerlov, (1974)

Previous (and current) developments, cont'd

K.J. Voss 1988 → present : Fish Eye camera coupled with a CID (then a CCD) matrix and spectral filters, and further polarization capabilities (successive versions: RADS, RADS-II, NURADS, POLRADS)

Voss K.J., 1989, SPIE Proc., 28(3), 241-247.
Voss K.J. and G. Zibordi, 1989, JAOT 6(4)652-662.
Morel, A., Voss, K.J. and B. Gentili (1995), J. Geophys. Res. 100, 13,143-13,150.
Voss K.J. and A. Chapin, 2005, Optics Express 13(11), 4250-4262.
Voss, K., Morel, A. and D. Antoine, 2007. Biogeosciences, 4, 781-789.
Voss K.J. and N. Souaïdia, 2010, Optics Express 18(19), 19762-19680.

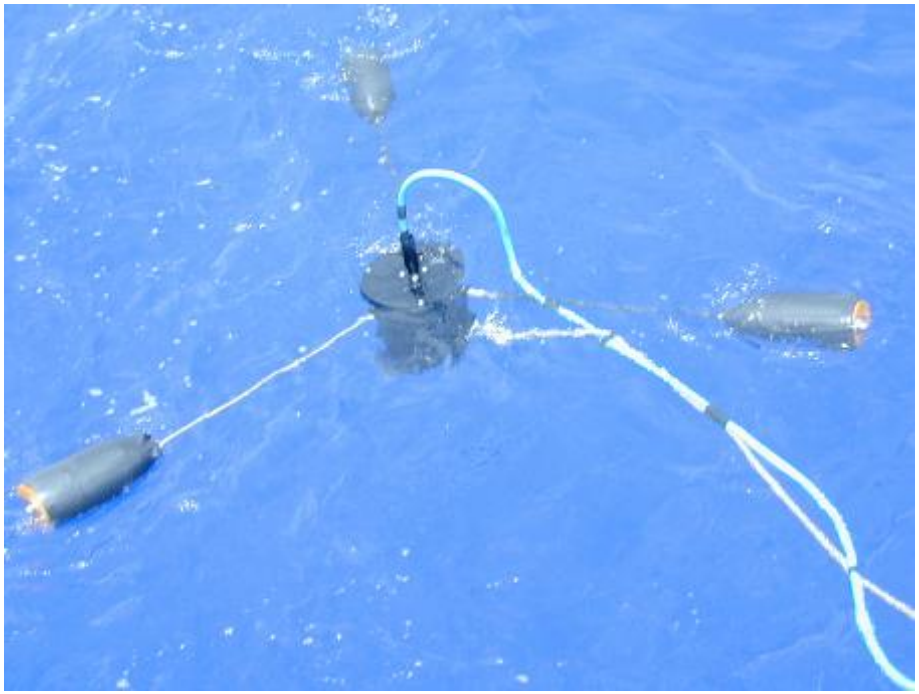

Our new development

Rationale / constraints

- There is a need to further document $L(\Xi_u)$ just beneath the surface

- There is a need to measure the complete distribution $L(\Xi)$ at depth

- Need for a dedicated fisheye optics

- Further miniaturization (self-shading)

- Being able to measure the 2 hemispheres simultaneously at various depths in the lit layers of the ocean

- Multi-spectral (across the visible)

- Budget-constrained (preventing to use high-level scientific CCD / CMOS)

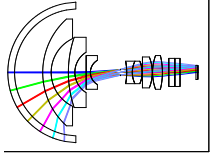

Our new development

406
438

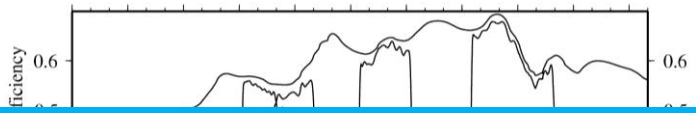

“CE-600” radiance camera system

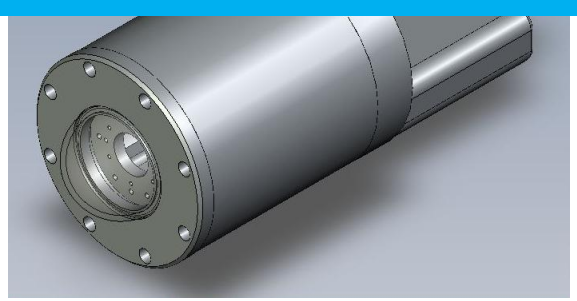

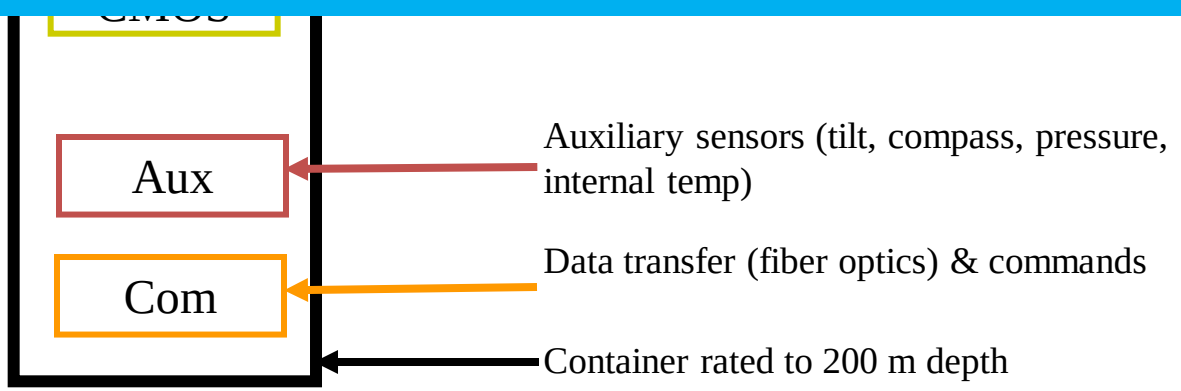

Radiometric characterization / calibration

Includes many steps:

- Linearity, dynamic range
- SNR determination
- Angular resolution
- Geometrical projection
- Spectral characterization
- Relative "rolloff" function of the fisheye
- Residual sensitivity to polarization
- Immersion factor
- Absolute radiometric calibration
- Straylight
- PSF

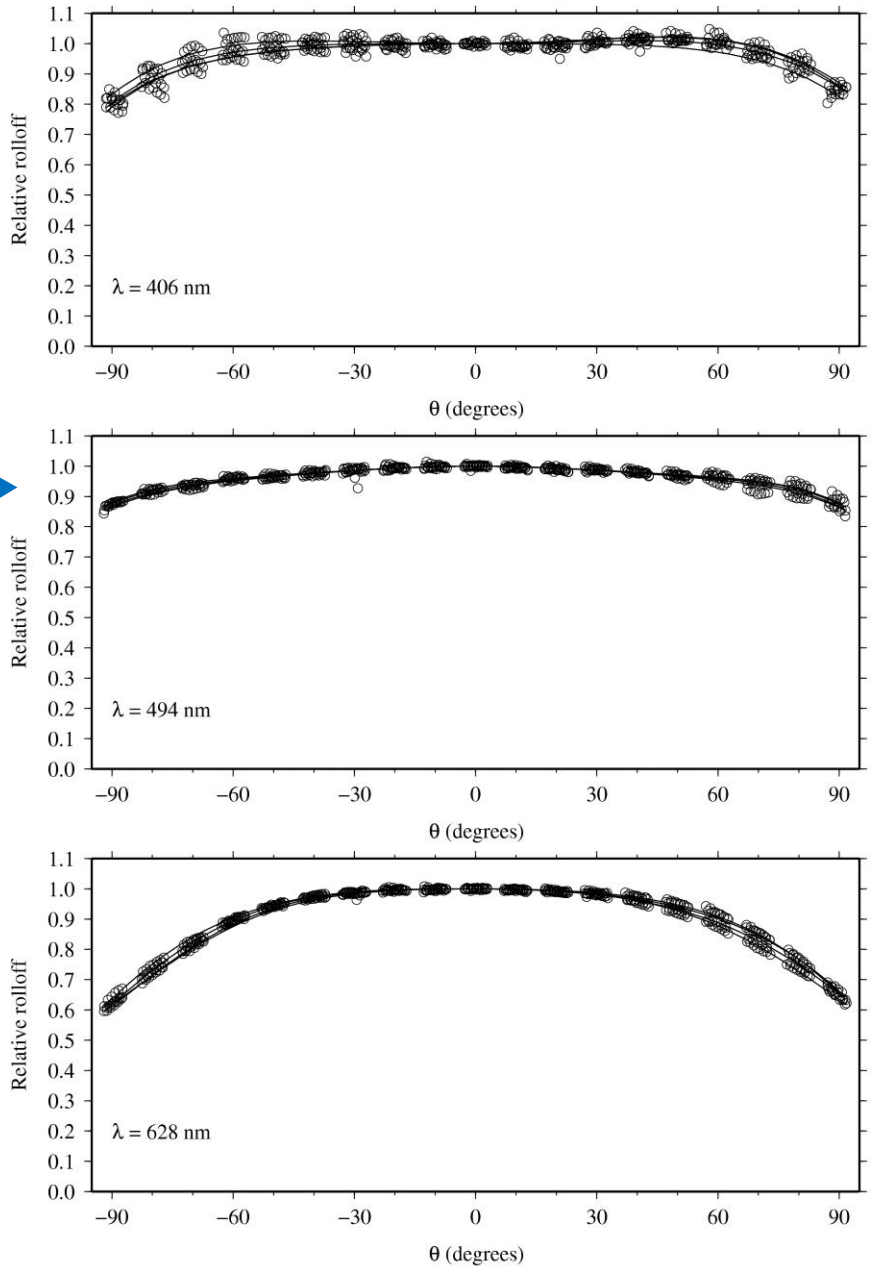

Most of these have been described elsewhere

(e.g.,
Voss and Zibordi, *1989*, JAOT 6(4)652-662;
Voss and Chapin, *2005*, Optics Express 13(11), 4250-4262)

Deployment modes

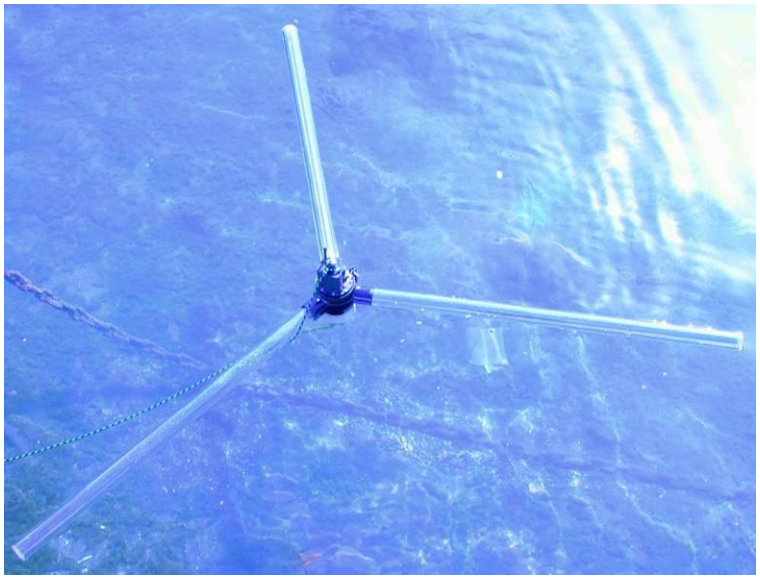

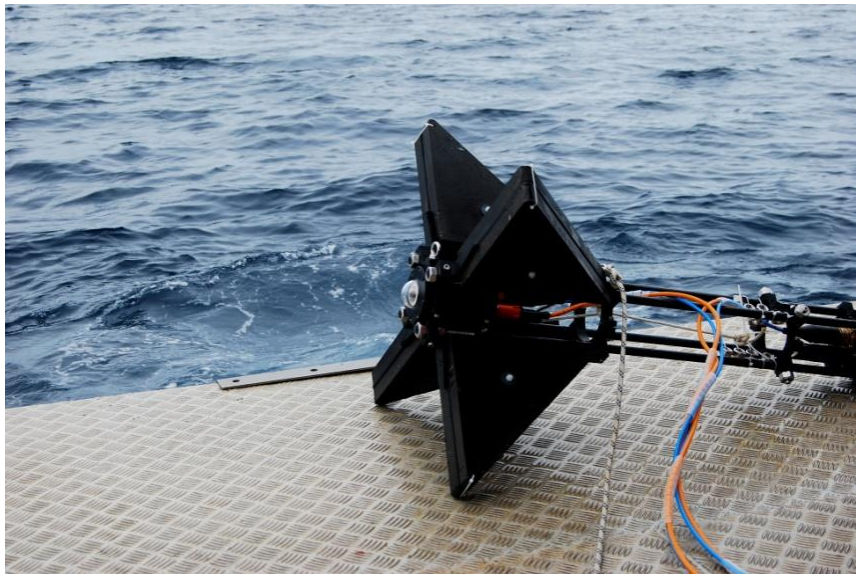

Surface mode:
$L(\Xi_u, 0^-)$

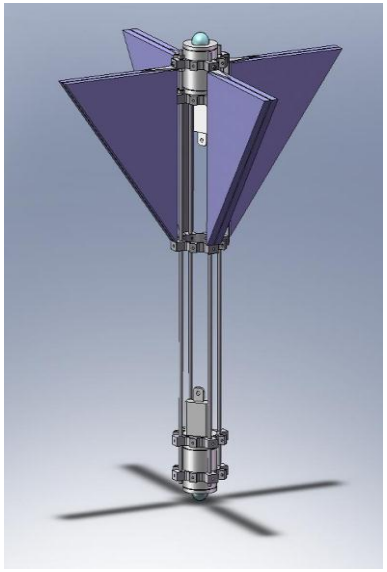

Profiling mode
(preliminary design):
$L(\Xi, z)$

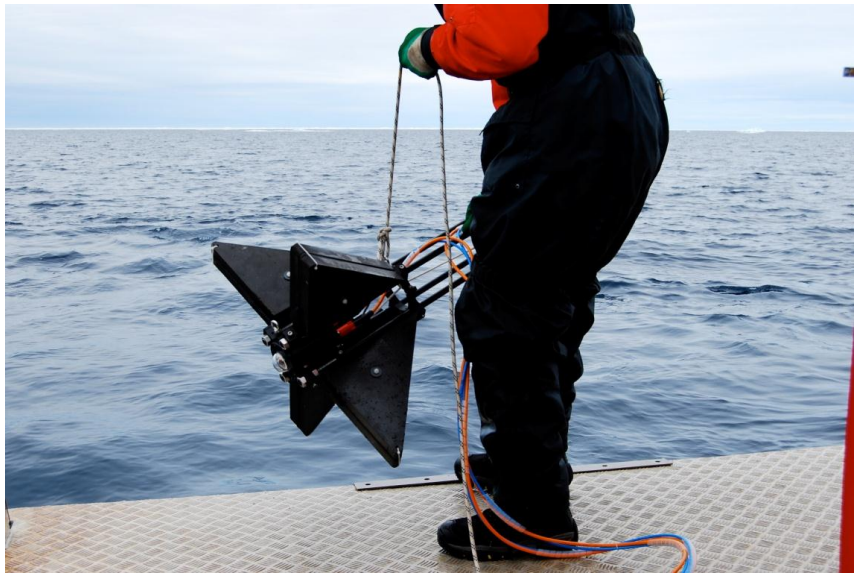

Sample results

$L(\Xi_u, 0^-)$

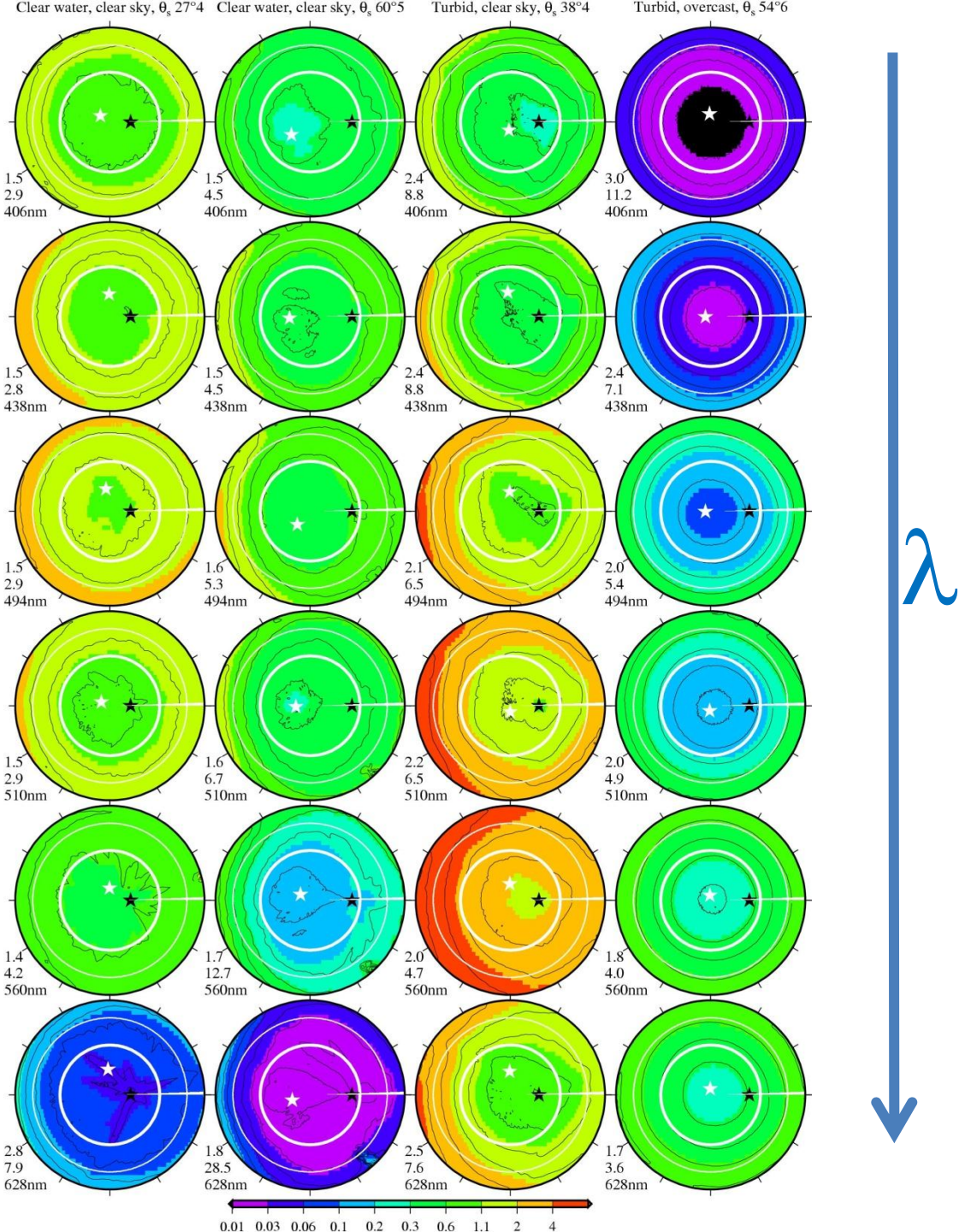

Full radiance distributions: L(Ξ, z)

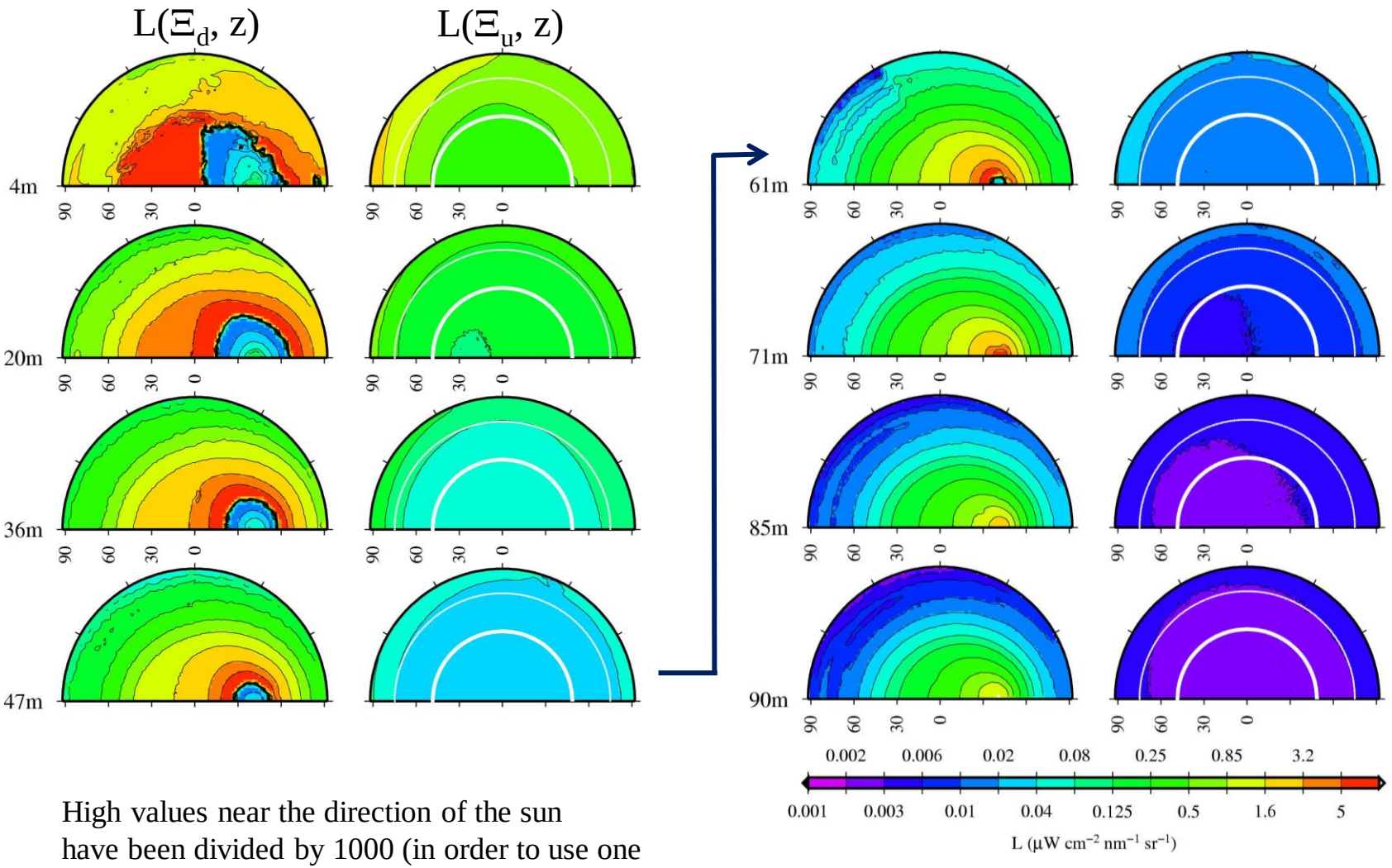

High values near the direction of the sun have been divided by 1000 (in order to use one single color scale for the entire plot)

λ=494 nm, clear waters (Chl~0.1 mg m^{-3}), sun zenith angle ~65° in air (Arctic)

Validation against more classical in-water radiometers

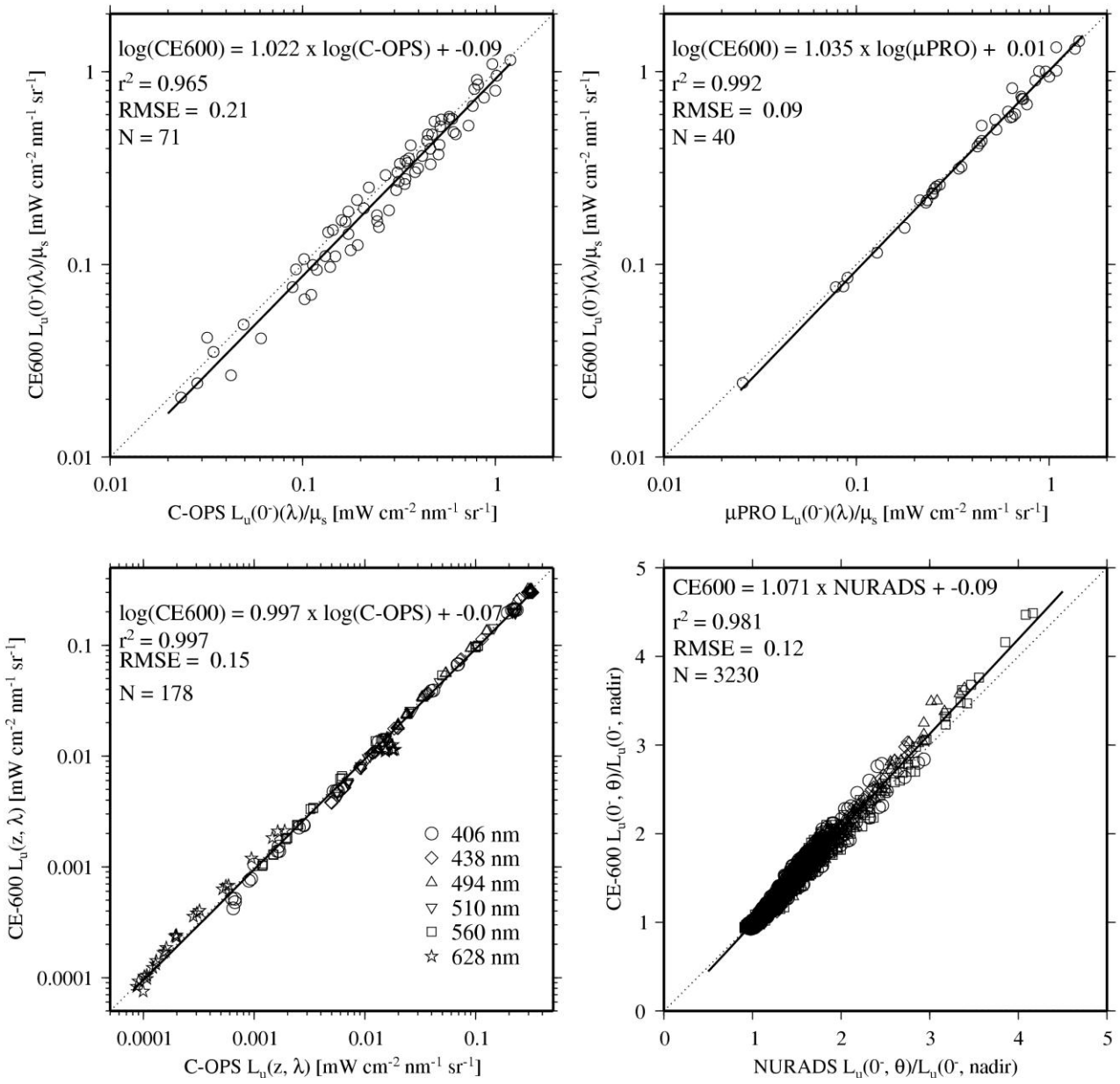

Tentative inversion of L(Ξ) in terms of optical properties: method

Starting from L(Ξ, z):

$$E_{0d}(z) = \int_{\phi=0}^{2\pi} \int_{\theta=0}^{\pi/2} L(z,\theta,\phi)\, d\omega \qquad E_{0u}(z) = \int_{\phi=0}^{2\pi} \int_{\theta=\pi/2}^{\pi} L(z,\theta,\phi)\, d\omega \qquad \text{and} \qquad E_0(z) = E_{0u}(z) + E_{0d}(z)$$

$$E_d(z) = \int_{\phi=0}^{2\pi} \int_{\theta=0}^{\pi/2} L(z,\theta,\phi)\ \cos(\theta)\, d\omega \qquad E_u(z) = \int_{\phi=0}^{2\pi} \int_{\theta=\pi/2}^{\pi} L(z,\theta,\phi)\ \cos(\theta)\, d\omega$$

$$a(z)\, E_0(z) = -\frac{d\left[E_d(z) - E_u(z)\right]}{dz}$$ *Gershun (1939) equation; Preisendorfer (1976)*

$$K(\pi,z) = -\frac{1}{L(\pi,z)} \frac{dL(\pi,z)}{dz} \qquad \text{and} \qquad RSR(z) = \frac{L(\pi,z)}{E_{0d}(z)}$$

$$b_b(z) = \frac{RSR(z)\left[K(\pi,z) + a(z)\right]}{(1/2\pi) - RSR(z)}$$

$$\frac{a}{K_\infty} = \frac{1-(b/c)}{1-0.52(b/c)-0.44(b/c)^2} \quad \text{and then} \quad b = a\left[\frac{b/c}{1-(b/c)}\right]$$ where K_∞ is derived from K_E at several depths

Zaneveld, R.J.V., 1989, An asymptotic closure theory for irradiance in the sea and its inversion to obtain the inherent optical properties, ***Limnology and Oceanography*** *19, 1442-1452.*

Tentative inversion of L(Ξ): results

λ=494 nm, clear waters (K_d~0.1 m^{-1}), θ_s in air ~ 65° (Arctic)

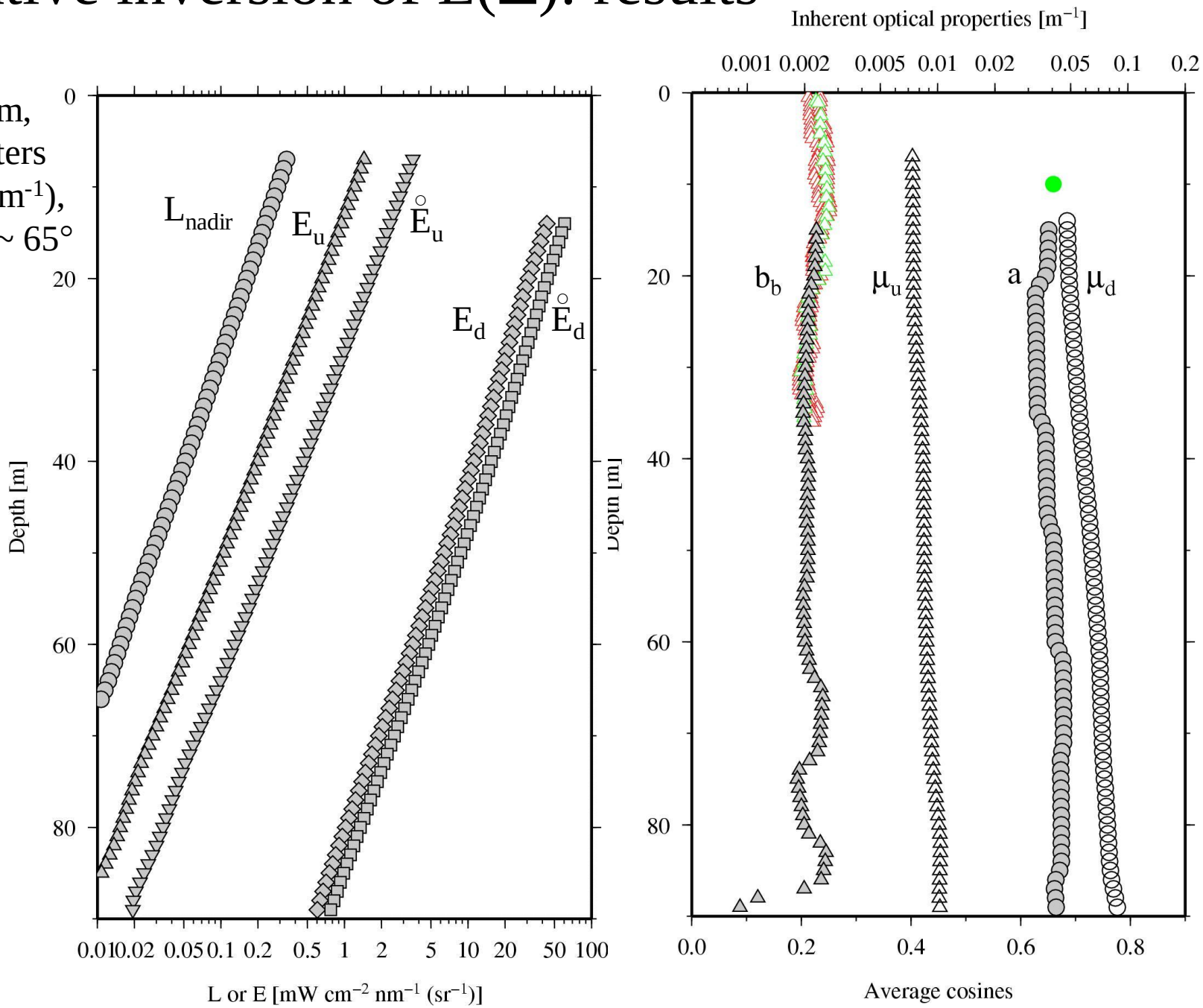

Conclusions / perspectives

- For the first time, we can measure vertical profiles of in-water L(Ξ) in several spectral bands and with high radiometric accuracy

- The instrument is validated against classical in-water radiometers

- Initial tests of the inversion procedure are very encouraging

- These results open the way for a totally new way of measuring optical properties in the ocean in a fully consistent way

- Improvements already foreseen:
  - Profiling system allowing low speed descent in the water column
  - Add a small cosine collector to help calibrating $E_d(\lambda)$
  - Improve calibration for high radiances (downwelling radiances)
  - Simultaneous measurement of the sky radiance

- Modifications in view of measuring sky radiances
  - Better thermal control (radiator)
  - Narrower filters
  - No need for the glass dome?

Improved design for the 2-camera profiling system

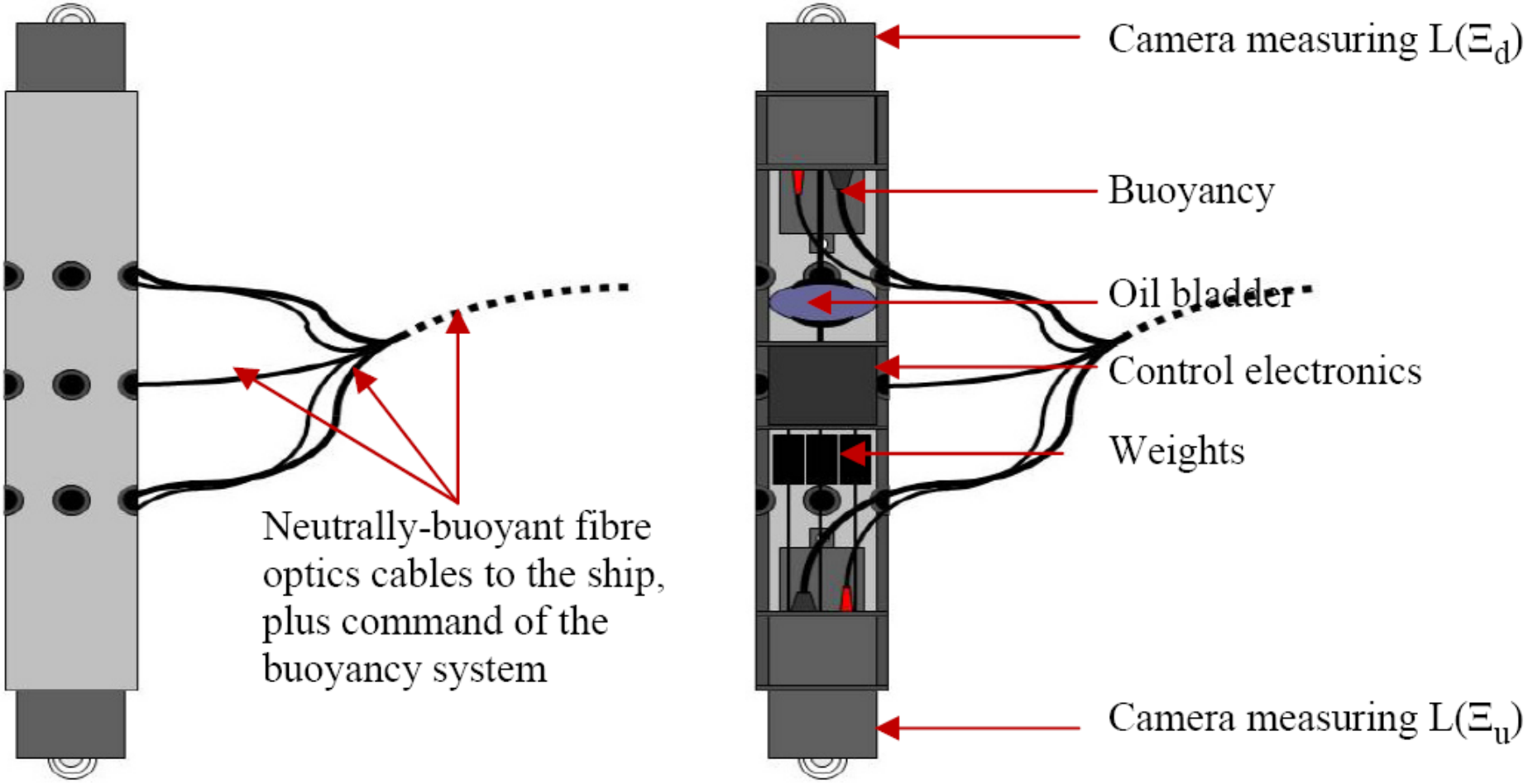

Thank you
for your attention

Backup

Noise characteristics of the CMOS array

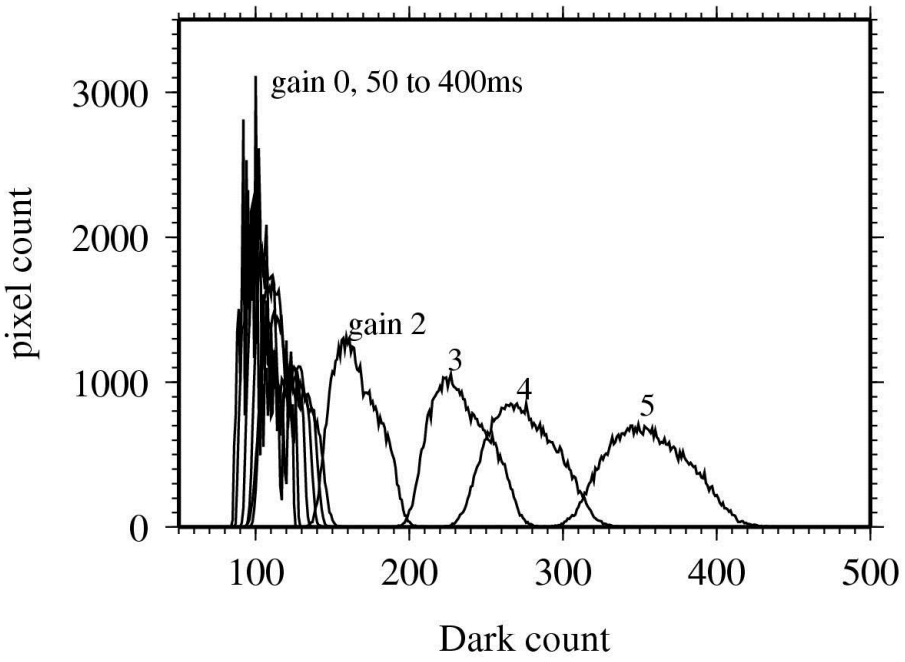

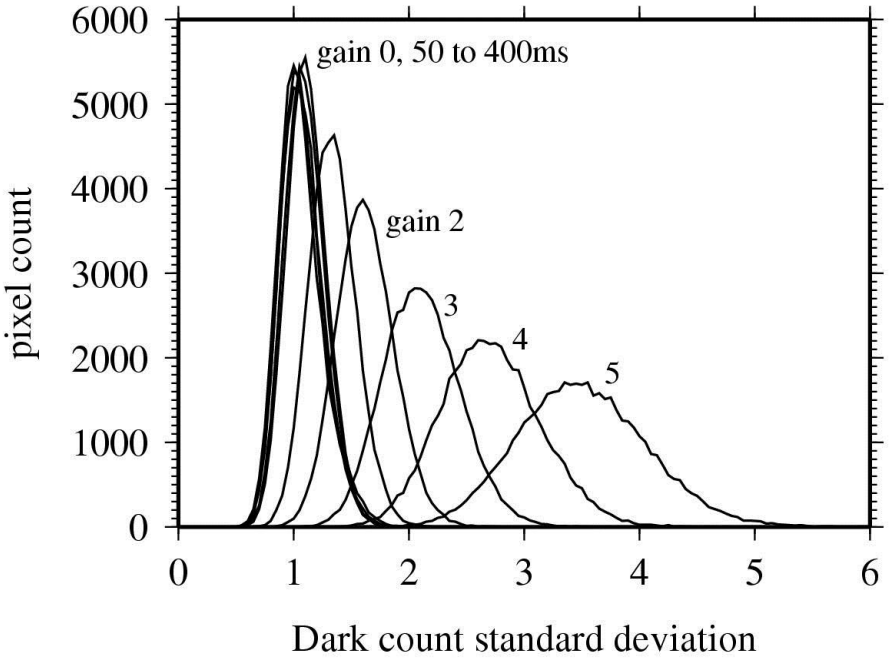

Spectral bands and detector QE

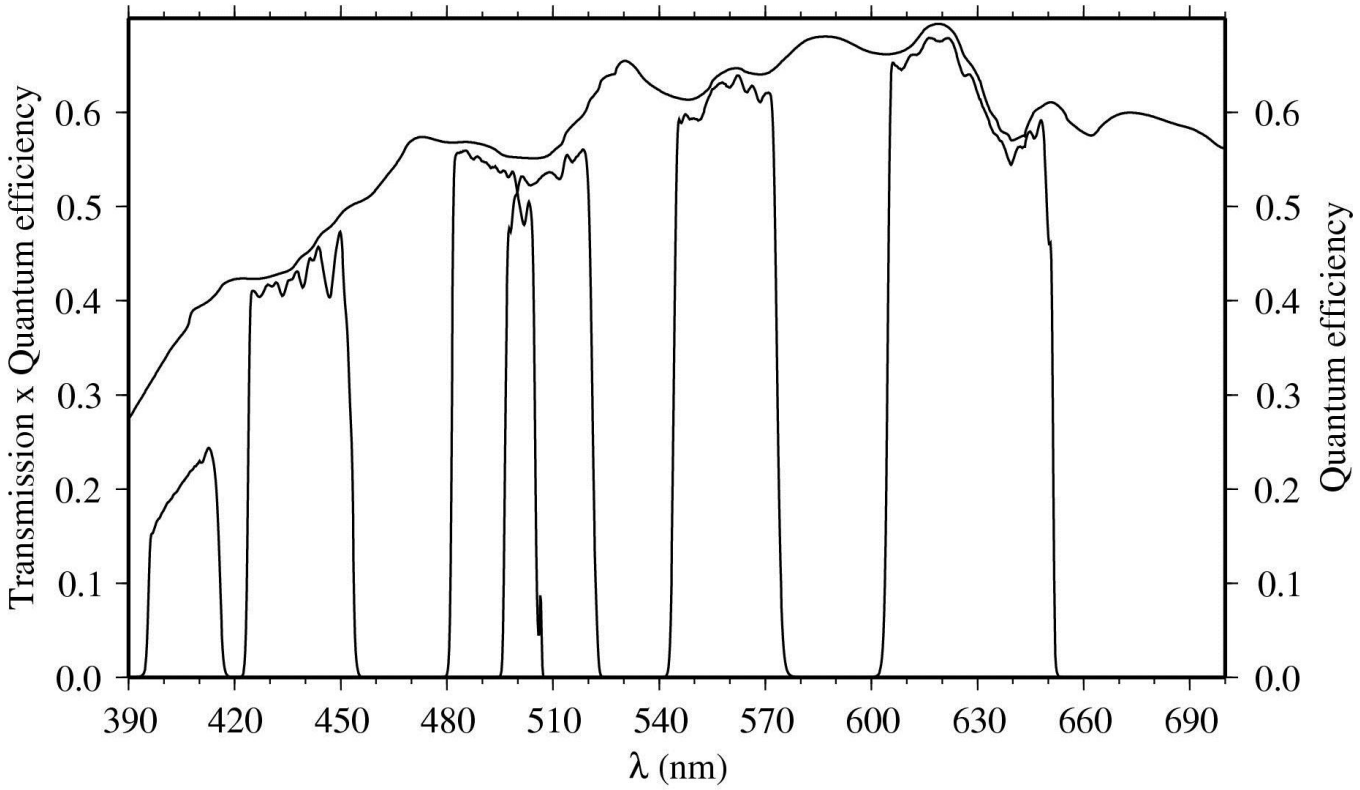

What was done before?

Jerlov N.G. and M. Fukuda, 1960, Tellus 12, 348-355

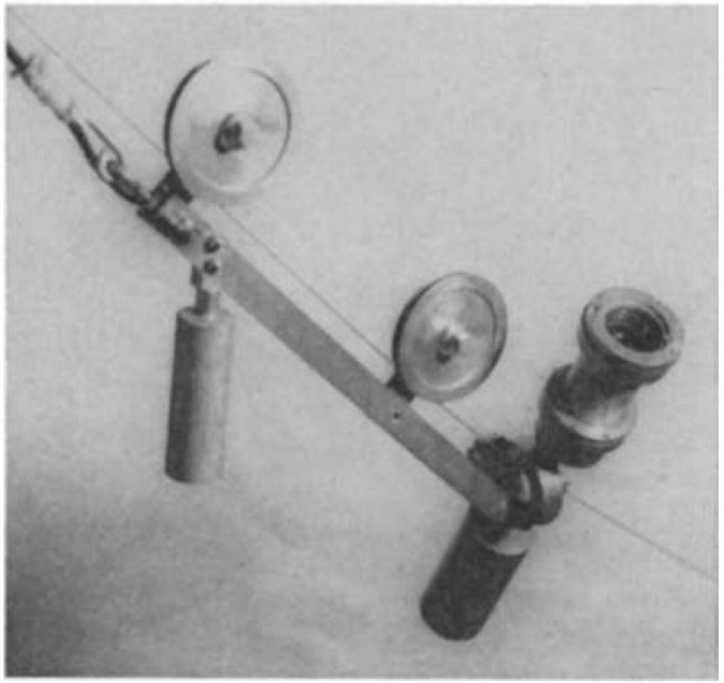

λ=535 nm

Gullmar Fjord, Norway

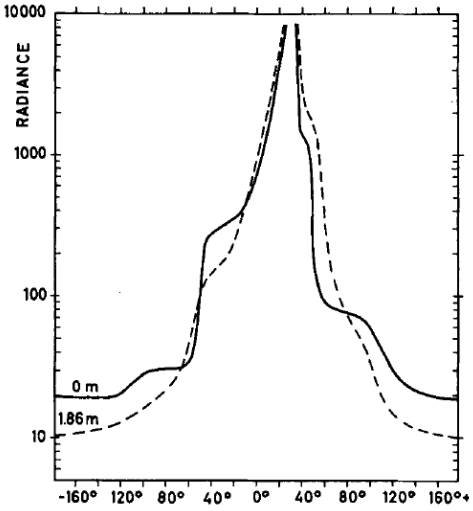

Fig. 3. Angular distribution of observed radiance (53 mμ) at surface and at 1.86 m depth.

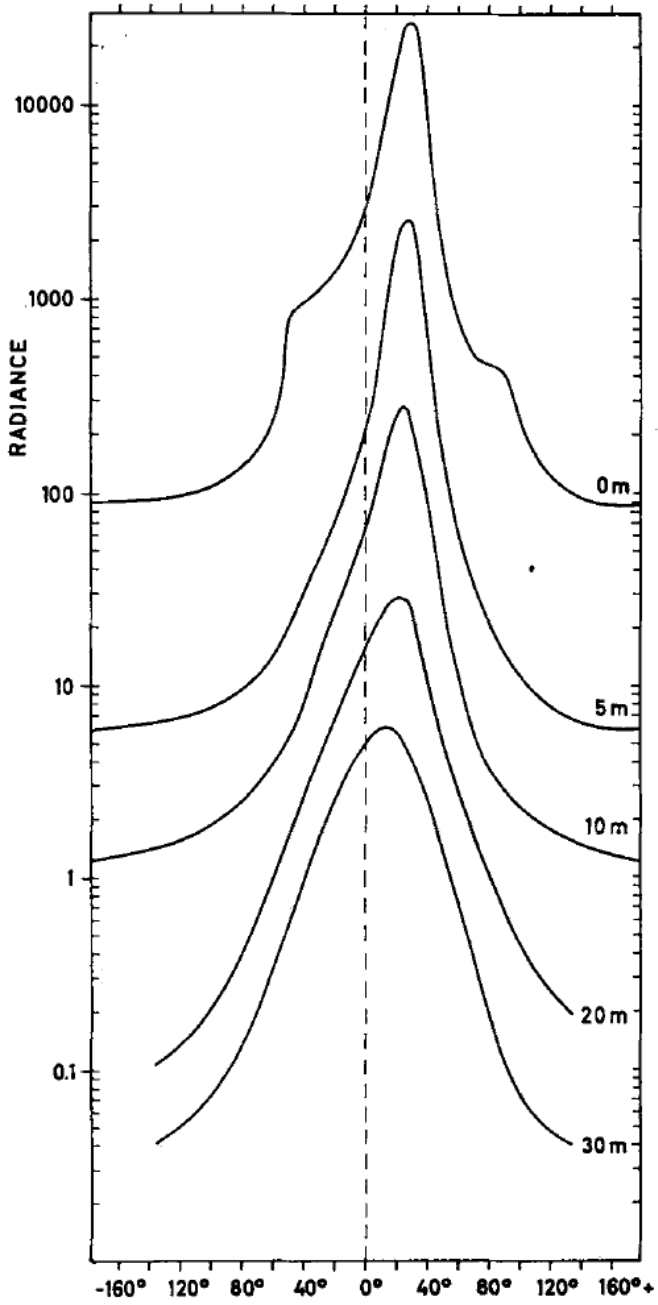

Fig. 4. Angular distribution of observed radiance (535 mμ) followed down to 30 m depth in order to illustrate the approach to a distribution symmetrical round the vertical.

What was done before?

Sasaki T. et al., 1962, Bull. Jap. Soc. Sci. Fish. 28(5), 489-496

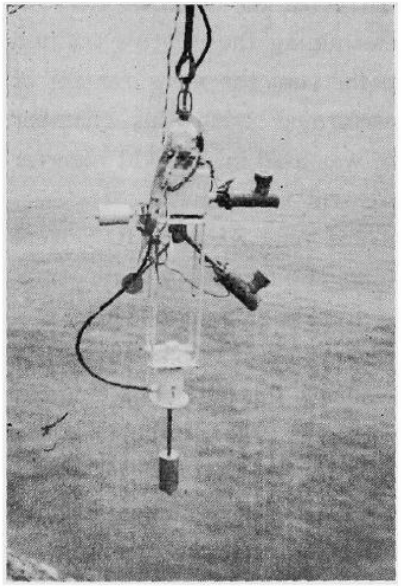

Fig. 1. The submerged unit before lowering.

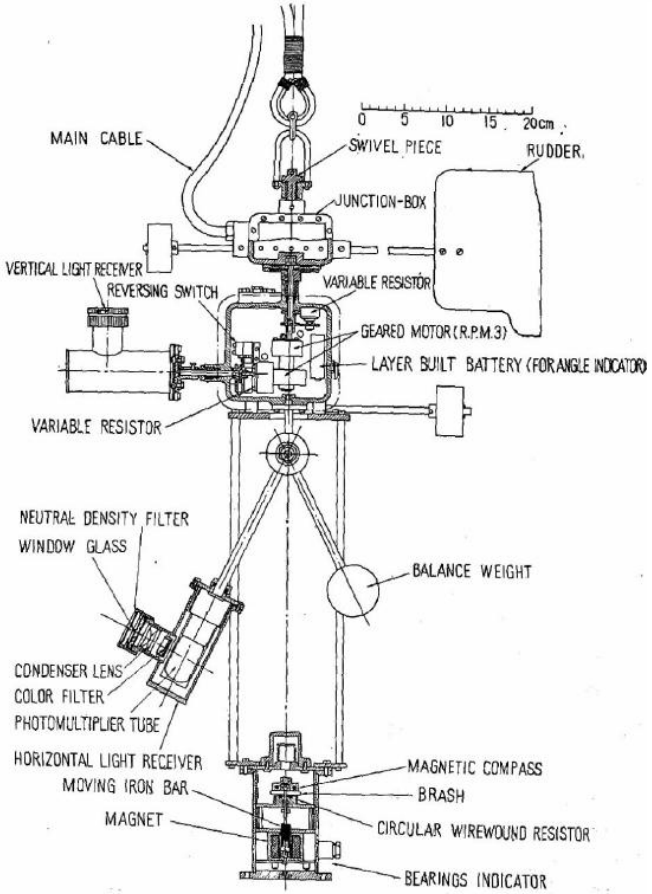

Fig. 2. General arrangement of the submerged unit.

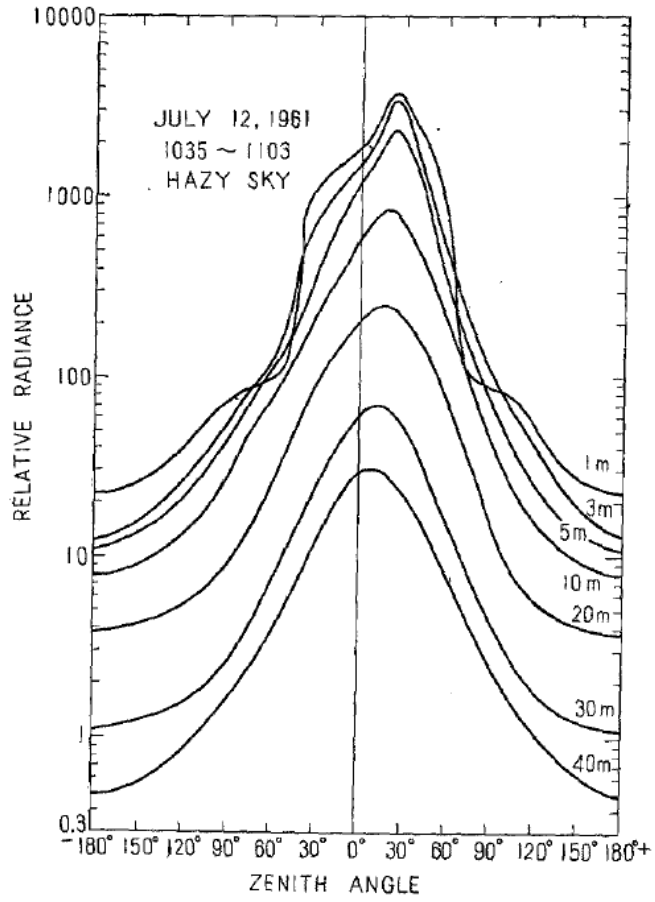

Fig. 8. Angular distributions in the vertical plane including the sun at the depths down to 40 m below the surface.

Measured off Ito city, Japan

λ~500 nm (100 nm wide)

What was done before?

John E. Tyler, 1960, Bull. Scripps Inst. Oceanogr. 7, 363-412.

Unidirectional photometer with elevation scanning

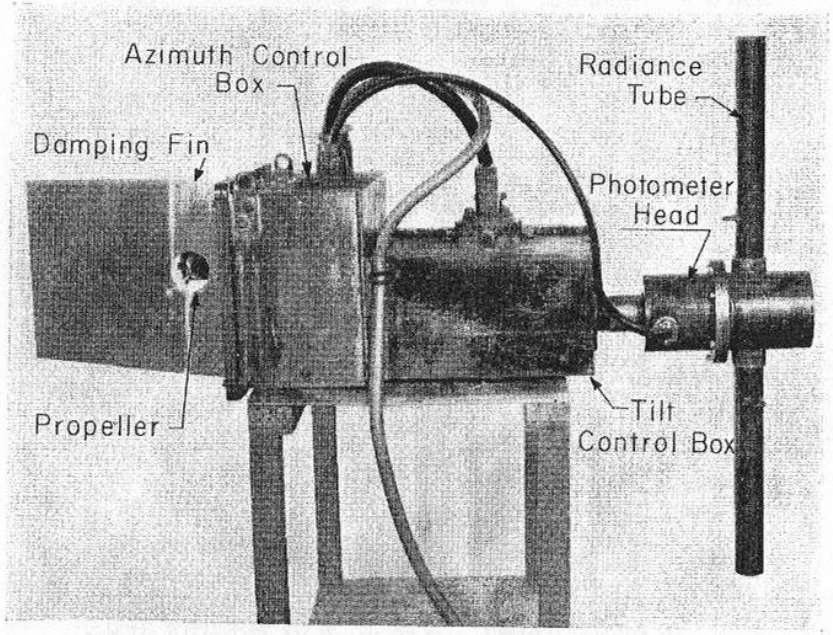

Fig. 8. Underwater radiance photometer (Tyler, 1960). The measuring head with its radiance tubes is on the right. The center box holds the tilt motor. The left box contains the gyrosyn compass and propeller-drive motor. The propeller can be seen through a hole in the damping fin on the left.

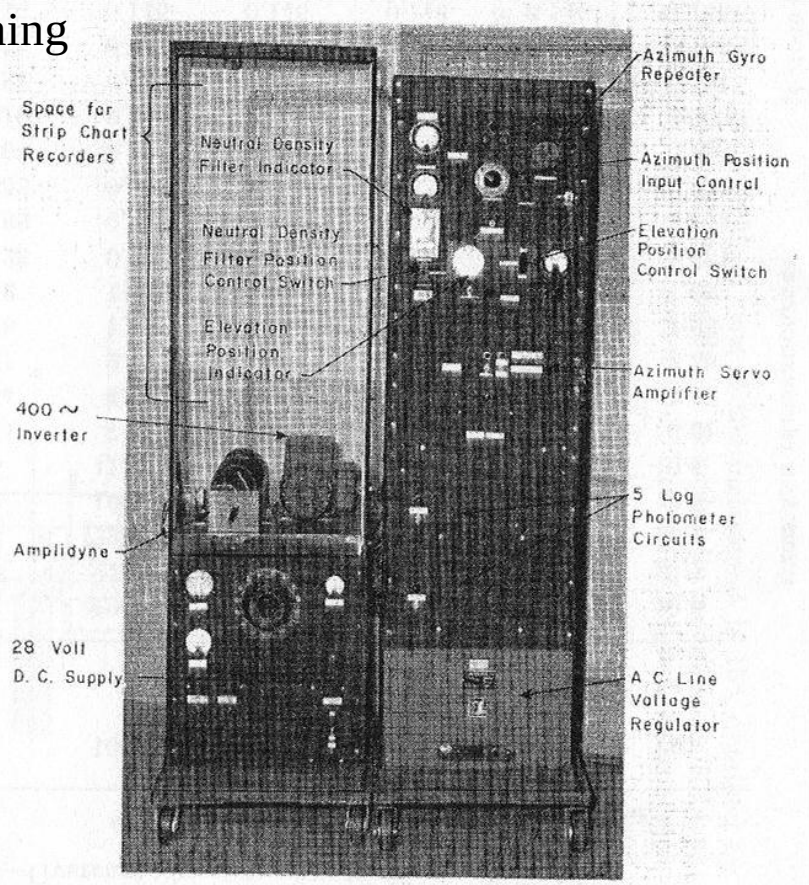

Fig. 9. Power supply and control panel for the underwater radiance photometer.

The Sea, Vol 1., M. N. Hill Ed., (1962)

Radiances distribution in Lake Pend'Oreille

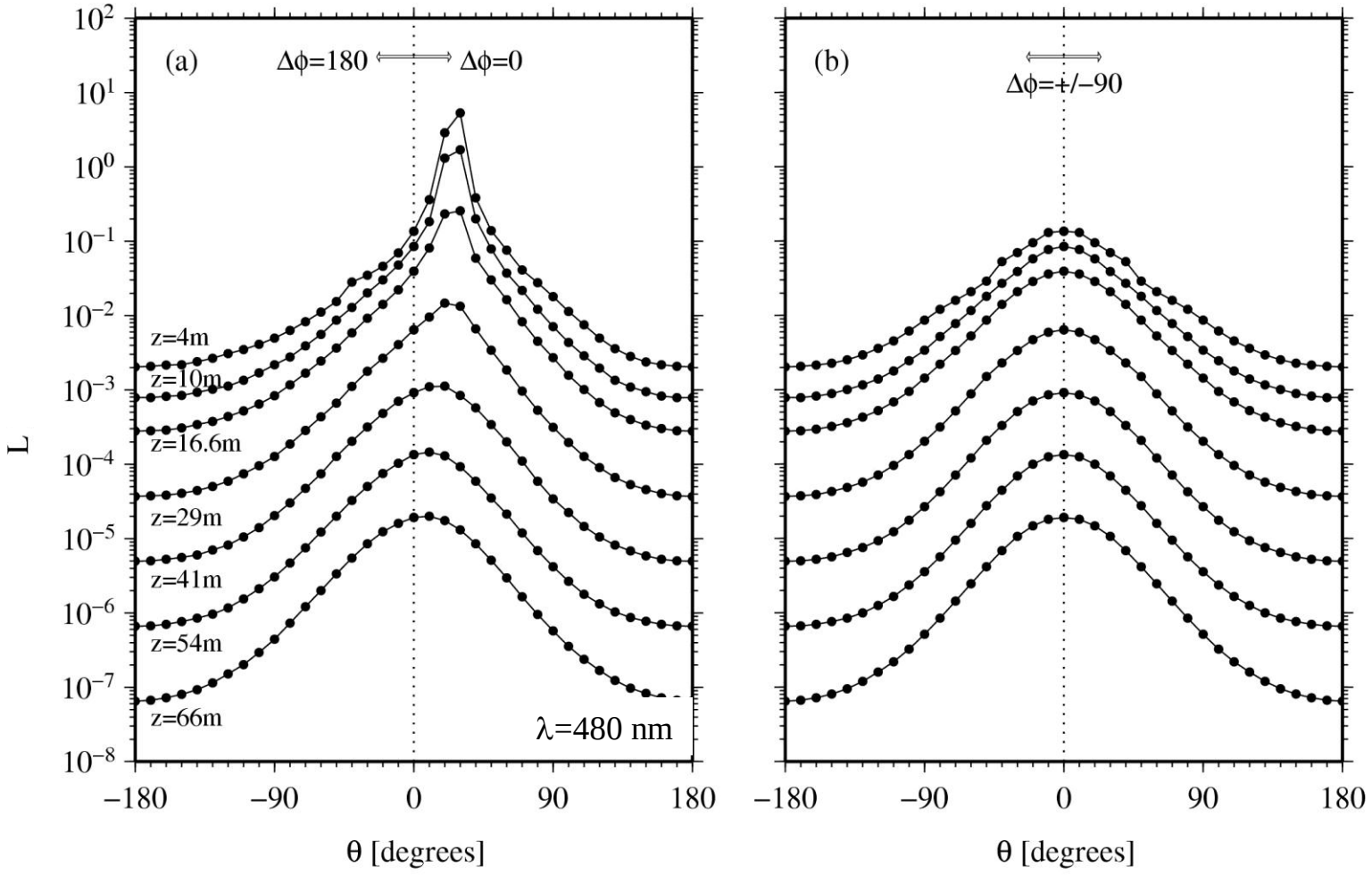

Principal plane

Perpendicular plane

Redrawn from the data published by Tyler, 1960

Previous developments, cont'd

R.C. Smith 1970 : Fish Eye camera

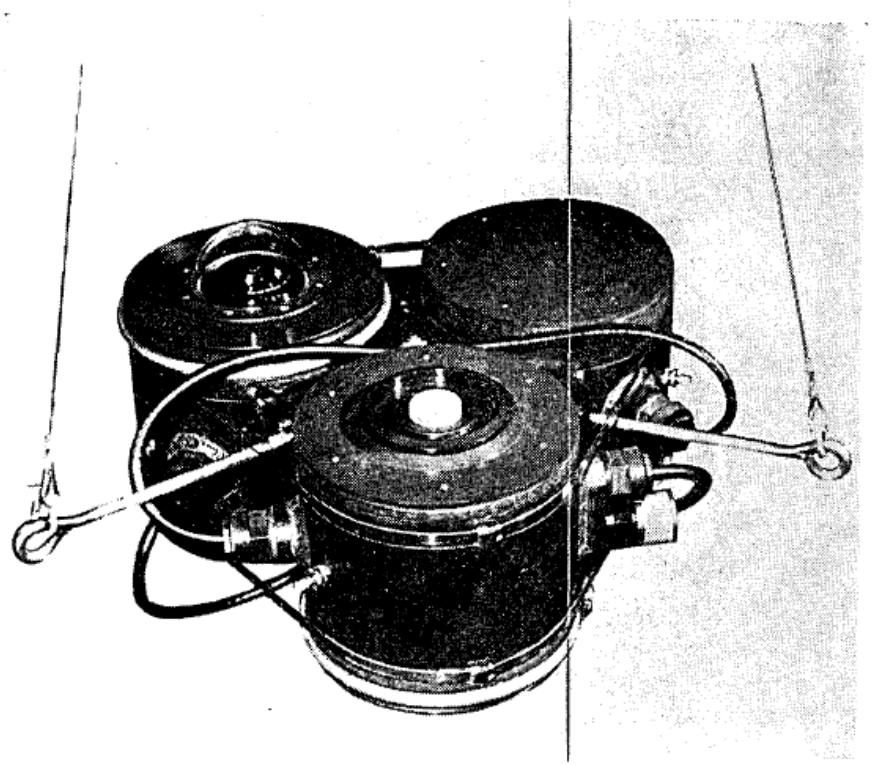

Smith R.C., R.W. Austin, and J.E. Tyler, 1970.
An oceanographic radiance distribution camera system, Applied Optics 9(9), 2015-2022

Previous developments, cont'd

Images taken by the Smith et al. camera system

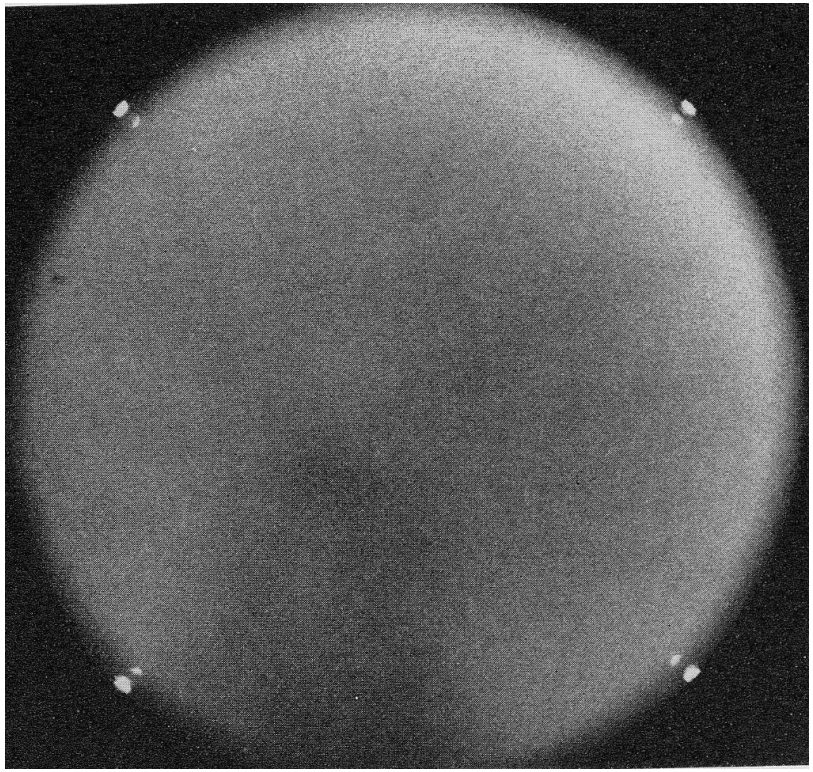

Upwelling radiances (Med. Sea 1972)

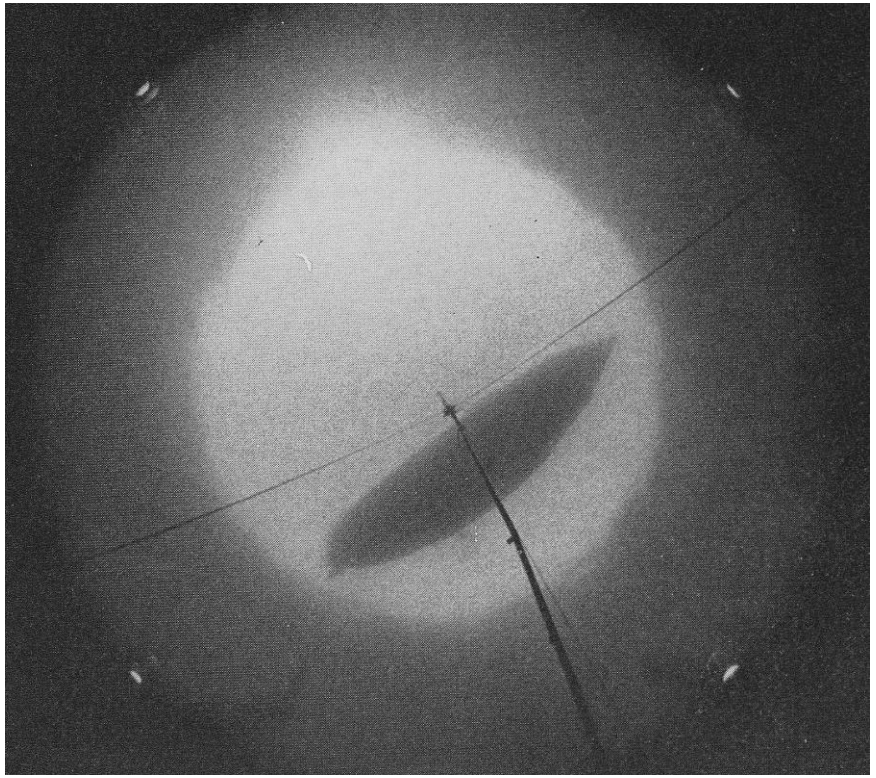

Downwelling radiances (Med. Sea 1972)

Optical Aspects of Oceanography, N.G. Jerlov, (1974)

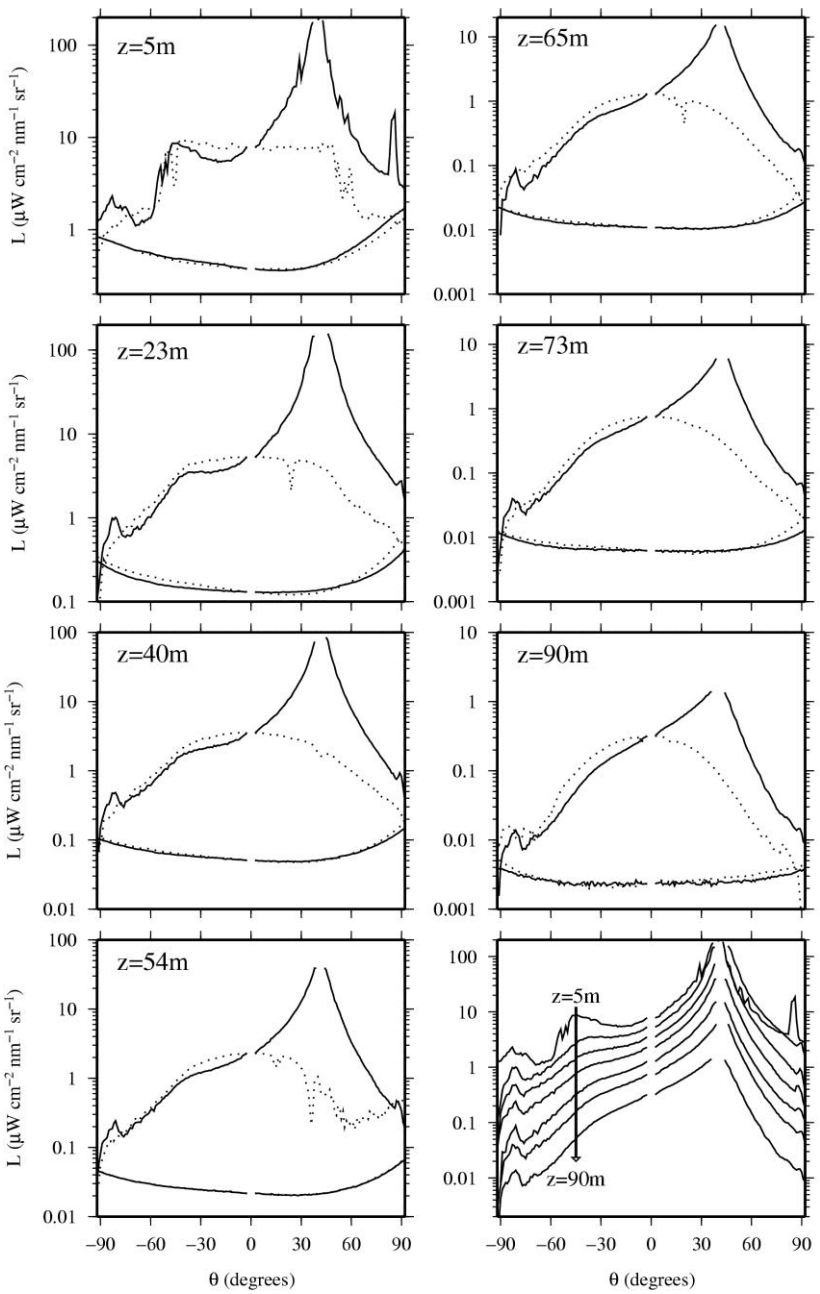

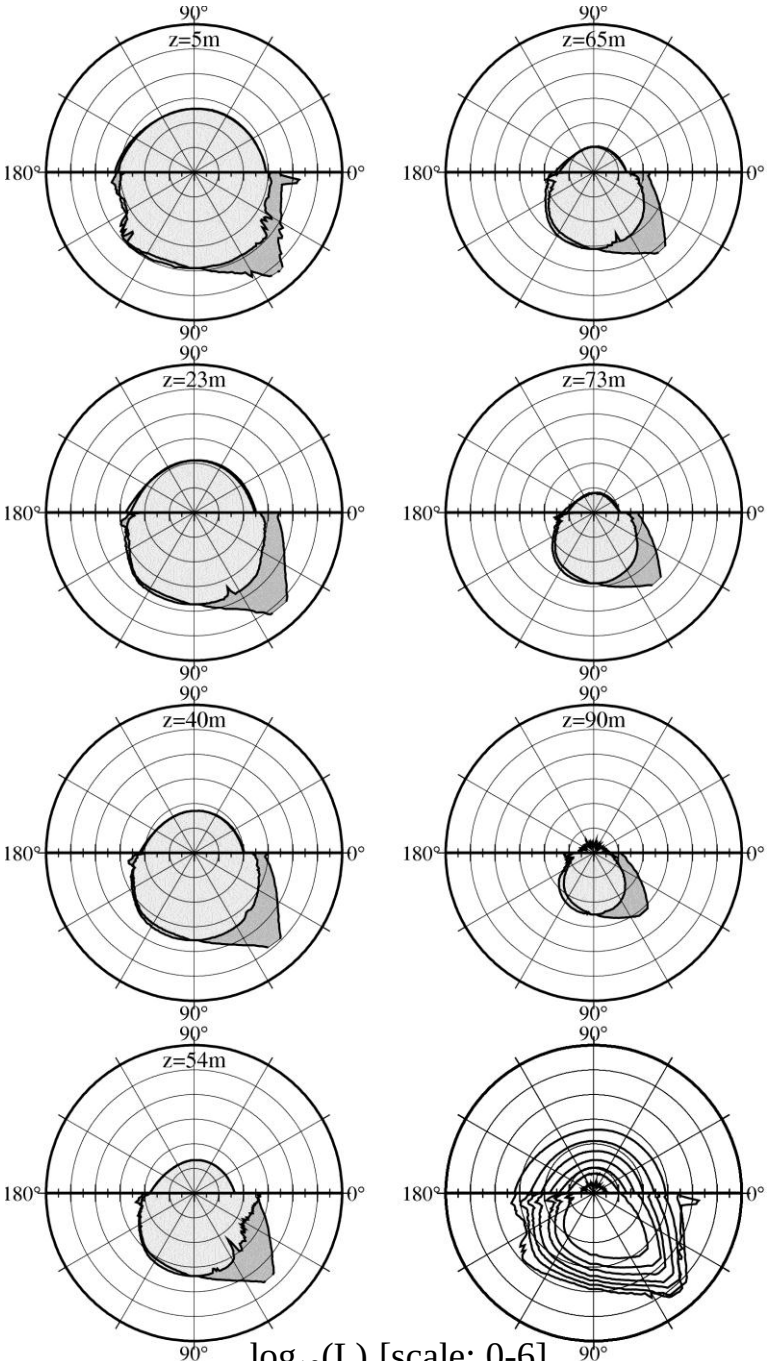

Full radiance distributions

$\log_{10}$(L) [scale: 0-6]
x1000 for upwelling radiances

Previous (and current) developments, cont'd

Measurements of the in-water radiance field

Med. Sea, AOPEX cruise, August 2004

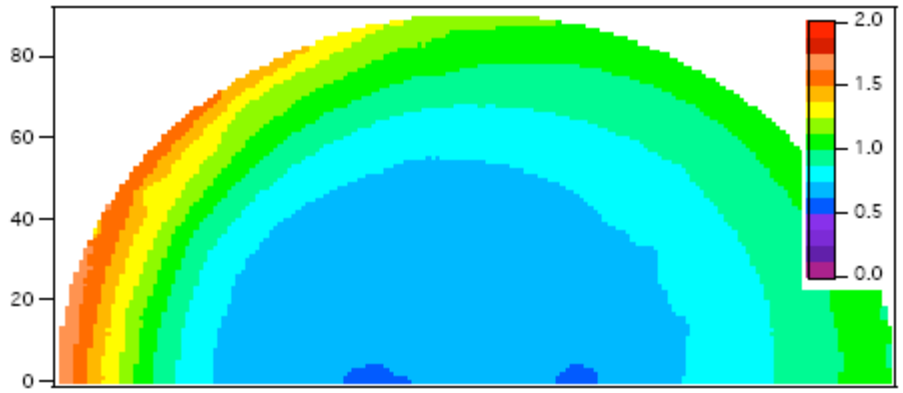

Radiance, average of 4 images

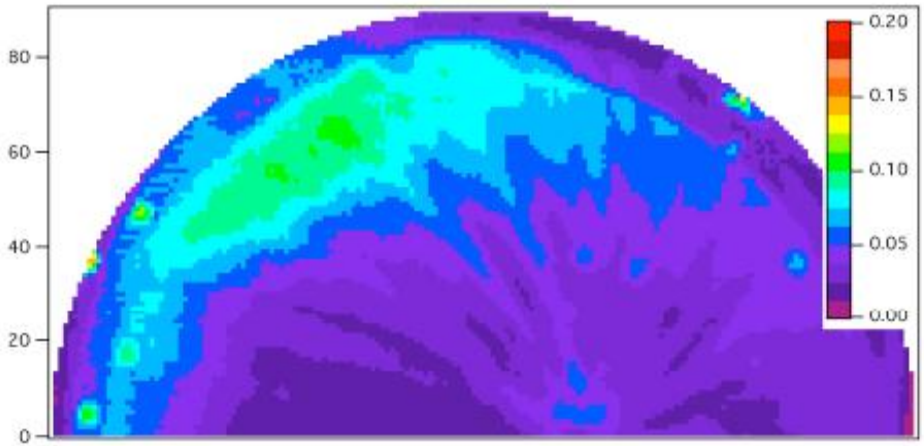

σ, determined on the 4 images

From Voss, K., Morel, A. and D. Antoine, Biogeosciences, 4, 781-789

CMOS characteristics

Technology Node	UMC 0.25 μm technology for CMOS Imaging Sensors
Resolution	1936 x 1090 visible pixels, 4 black rows, 72 black columns
Optical Format	2/3-inch (HDTV 1080p or Extended Sensitivity 720p)
Pixel Area	5 μm by 5 μm
Pixel rate	Nominal 150 MHz or 74.25 MHz (SMPTE 274M)
Image Capture	Electronic Focal Plane Rolling Shutter
Supply voltage	3.3 V analog and 2.5 V digital
Power consumption	<650 mW
Gain	Two analog gain stages with gain ranges of 0 → +24 dB and –6 → +18 dB, respectively, adjustable in 3 dB steps One digital gain stage (multiplier) with gain range of –24 dB to +72 dB, adjustable in 0.006 dB and 6 dB steps
Random Noise (rms)	5 LSB
Saturation Capacity	> 50 ke-
Dynamic Range	68 dB (>11 bits)

Noise characteristics

	406	438	494	510	560	628
Radiance ($\mu W\ cm^{-2}\ nm^{-1}\ sr^{-1}$)	0.047	0.075	0.14	0.16	0.23	0.32
Gain	5.1	2.8	2	2.8	1	1
Exposure (ms)	400	400	370	360	360	160
Standard deviation ($\mu W\ cm^{-2}\ nm^{-1}\ sr^{-1}$)	3.03×10^{-4}	2.04×10^{-4}	2.67×10^{-4}	4.07×10^{-4}	2.67×10^{-4}	3.73×10^{-4}
SNR	154	370	529	393	848	848
Dark counts	365	240	167	234	121	109
Useful dynamics (counts)	3672	3816	3897	3822	3951	3963